Received: 16 March 2020 | Revised: 29 September 2020 | Accepted: 1 October 2020

DOI: 10.1002/jnr.24743

RESEARCH ARTICLE

Increased occurrence of pathological mitochondria in astrocytic perivascular endfoot processes and neurons of idiopathic intracranial hypertension

Per Kristian Eide[1,2] | Md Mahdi Hasan-Olive[1,2] | Hans-Arne Hansson[3] | Rune Enger[4,5]

[1]Department of Neurosurgery, Oslo University Hospital - Rikshospitalet, Oslo, Norway

[2]Institute of Clinical Medicine, Faculty of Medicine, University of Oslo, Oslo, Norway

[3]Institute of Biomedicine, University of Gothenburg, Göteborg, Sweden

[4]GliaLab and Letten Centre, Division of Anatomy and Division of Physiology, Department of Molecular Medicine, Institute of Basic Medical Sciences, University of Oslo, Oslo, Norway

[5]Department of Neurology, Oslo University Hospital - Rikshospitalet, Oslo, Norway

Correspondence
Per Kristian Eide, Department of Neurosurgery, Oslo University Hospital - Rikshospitalet, Pb 4950 Nydalen, N-0424 Oslo, Norway.
Email: p.k.eide@medisin.uio.no, peide@ous-hf.no

Funding information
Health South-East Norway, Grant/Award Number: 2012016 and 2016027

Abstract

Idiopathic intracranial hypertension (IIH) primarily affects fertile, overweight women, and presents with the symptoms of raised intracranial pressure. The etiology is unknown but has been thought to relate to cerebrospinal fluid disturbance or cerebral venous stenosis. We have previously found evidence that IIH is also a disease of the brain parenchyma, evidenced by alterations at the neurogliovascular interface, including astrogliosis, pathological changes in the basement membrane and pericytes, and alterations of perivascular aquaporin-4. The aim of this present electron microscopic study was to examine whether mitochondria phenotype was changed in IIH, particularly focusing on perivascular astrocytic endfeet and neurons (soma and pre- and postsynaptic terminals). Cortical brain biopsies of nine reference individuals and eight IIH patients were analyzed for subcellular distribution and phenotypical features of mitochondria using transmission electron microscopy. We found significantly increased prevalence of pathological mitochondria and reduced number of normal mitochondria in astrocytic endfeet of IIH patients. The degree of astrogliosis correlated negatively with the number of normal mitochondria in astrocytic endfoot processes. Moreover, we found significantly increased number of pathological mitochondria in pre- and postsynaptic neuronal terminals, as well as significantly shortened distance between mitochondria and endoplasmic reticulum contacts. Finally, the length of postsynaptic density, a marker of synaptic strength, was on average reduced in IIH. The present data provide evidence of pathological mitochondria in perivascular astrocytes endfeet and neurons of IIH patients, highlighting that impaired metabolism at the neurogliovascular interface may be a facet of IIH.

KEYWORDS

astrocytes, electron microscopy, idiopathic intracranial hypertension, mitochondria, neurogliovascular unit, neurons, pseudotumor cerebri, reduced postsynaptic density

Edited by Jerome Badaut and David McArthur. Reviewed by Wolfram Kunz and Keith Murai.

1 | INTRODUCTION

Idiopathic intracranial hypertension (IIH) is a disorder characterized by raised intracranial pressure (ICP) (Eide & Kerty, 2011; Fric & Eide, 2017; Winters & Kleinschmidt-Demasters, 2015), and a wide range of accompanying symptoms, such as headache, visual failure, tinnitus, olfactory dysfunction, cognitive impairment, and fatigue, typically affecting overweight women (Ball & Clarke, 2006; Kharkar et al., 2011; Kunte et al., 2013; Mollan et al., 2016; Yri et al., 2014). The burden of the disease is high for affected individuals who are usually young people (Friesner et al., 2011; Kleinschmidt et al., 2000). The occurrence of the disease is clearly on the rise, potentially due to the increasing weight of people in the Western world (Curry et al., 2005; Kesler et al., 2014; Raoof et al., 2011).

The cause of the elevated ICP in IIH remains unknown, but may be related to cerebrospinal fluid (CSF) disturbance with elevated CSF pressure and abnormal cerebral venous pressure due to dural vein stenosis (Mollan et al., 2016). Current treatment is not targeted toward the mechanisms underlying the development of IIH, but is rather symptomatic, with the goal of reducing ICP and symptoms related to increased ICP (Mollan et al., 2018). Treatments include weight reduction, medication to reduce CSF production (e.g., acetazolamide), and ultimately neurosurgery aiming at CSF diversion by shunt implantation. Another treatment option is stenting of dural vein stenosis if such changes are present, to reduce venous pressure and consequently ICP (Albuquerque et al., 2011). Unfortunately, current symptomatic treatments have significant shortcomings, which explain why many affected individuals have lasting complaints with frequent hospitalizations (Friesner et al., 2011).

Since IIH has not been considered a "brain" disease, rather a disease of the CSF or the intracranial venous system, little focus has been given to pathological changes within the brain parenchyma. In cortical brain biopsies of individuals with IIH, we have previously demonstrated patchy astrogliosis (Eide et al., 2016), changes in the basement membrane of cerebral capillaries and in pericytes (Eidsvaag et al., 2018), and leakage of blood proteins over blood–brain barrier (BBB) (Hasan-Olive et al., 2019). Using CD68 labeling, we found no evidence for microglia/macrophage activation (Eide et al., 2016).

Astrocytes, the main glial cell type in gray matter, are involved in a wide range of brain pathologies. In the healthy brain astrocytes are key homeostatic controllers of the extracellular space, and accruing evidence also suggests they more actively partake in information transfer in neuronal networks (Verkhratsky & Nedergaard, 2018). Astrocytic endfeet are specialized processes that near completely ensheath the vasculature in the brain, exhibiting a rich repertoire of signaling patterns, which are presumed to serve important functions related to vasomotion and water homeostasis (Boulay et al., 2017; Langer et al., 2017; Mulligan & MacVicar, 2004). In the diseased brain, however, astrocytes change their tasks to reparative processes by a transformation of morphology and function known as reactive gliosis (Pekny & Pekna, 2014). This process also affects the astrocytic endfeet, and the molecular composition of endfeet has been shown to be disturbed in several brain diseases characterized by reactive gliosis (Eid et al., 2005; Heuser et al., 2012).

Significance

Electron microscopy of cortical brain biopsies from idiopathic intracranial hypertension (IIH) patients and controls showed in IIH increased prevalence of pathological mitochondria in astrocytic endfeet, as well as in pre- and postsynaptic neuronal terminals, shortened distance between mitochondria and endoplasmic reticulum and reduced postsynaptic density.

Astrocytic perivascular endfeet are of particular interest in the context of IIH as they are hypothesized to be important in the regulation of the exchange of CSF between perivascular spaces and the brain parenchyma (Iliff et al., 2012), and play an important role in brain water homeostasis (Amiry-Moghaddam & Ottersen, 2003). We have previously shown that alterations at the neurogliovascular interface, including astrogliosis (Eide et al., 2016), pathological changes in the basement membrane and pericytes (Eidsvaag et al., 2018), and alterations of perivascular aquaporin-4 (Eide et al., 2016) are hallmarks of IIH. To support the complex functions and signaling patterns of endfeet, the endfeet would need well-functioning mitochondria. Mitochondria plays an imperative role in balancing energy demand and cell death in the brain (Kirschen et al., 2018). To the best of our knowledge, there are currently no reports on mitochondrial health in astrocyte endfeet in IIH. With this background, the aim of the present study was to examine for pathological changes of astrocytic endfoot mitochondria in brain biopsies of IIH patients. The present study demonstrates, for the first time, significant pathological changes to astrocyte endfoot mitochondria in patients with IIH. Our findings suggest that perturbed metabolism of the organism (overweight) and perturbed brain cell energy metabolism goes hand-in-hand and that pathology of astrocytic endfeet play a role in IIH.

2 | MATERIALS AND METHODS

2.1 | Ethical approvals

The study was approved by The Regional Committee for Medical and Health Research Ethics (REK) of Health Region South-East, Norway: (a) Brain Tissue Research Biobank (Approval no. REK 2010/1030 & 2012/1157). (b) Brain biopsy from iNPH patients (Approval no. REK 2009/2060). (c) Storage of brain tissue from Ref patients, that is patients undergoing neurosurgery for various reasons (epilepsy, tumor, or cerebral aneurysms) wherein the removal of brain tissue is necessary as part of treatment (Approval no. REK 2011/2306). The study also was approved by Oslo University Hospital (Approvals no. 10/6806 and 2011/19311). The study was performed in accordance with the ethical standards as laid down in the 1964 Declaration of Helsinki and its later amendments or comparable ethical standards. Consecutive patients were included after oral and written informed consent.

2.2 | Experimental design

We used a prospective and observational study design; EM specimens were analyzed by a person (MMHO) who was blinded to patient data and diagnosis.

2.3 | Participants

2.3.1 | REF individuals

Reference (REF) subjects included patients who underwent neurosurgery for various reasons, in whom removal of normal brain tissue was part of the planned brain surgery: (a) Individuals undergoing brain tissue resection for epilepsy (six patients). (b) Individuals undergoing elective clipping of cerebral aneurysm (two patients). (c) Individuals undergoing tissue resection for brain tumor (one patient).

IIH patients

The IIH patients included consecutive patients referred to the Department of Neurosurgery, Oslo University Hospital - Rikshospitalet, Oslo, Norway, from local neurological and ophthalmological departments due to failed conservative treatment. They met the modified Dandy criteria (Friedman & Jacobson, 2002). The condition IIH was first described by Dandy and named pseudotumor cerebri (Dandy, 1937). It has been denoted pseudotumor cerebri, benign intracranial hypertension, or IIH, typically characterized by increased ICP, usually measured as elevated CSF pressure by lumbar puncture (Mollan et al., 2018). In this institution, all IIH patients undergo overnight ICP monitoring, which typically reveal elevated static and pulsatile ICP, as previously reported (Eide & Kerty, 2011; Fric & Eide, 2017).

2.4 | Sampling and handling of brain tissue

The brain tissue from IIH patients was sampled during placement of an ICP sensor for overnight ICP monitoring, which was performed in the operation room. A skin incision was made frontally on the right side in local anesthesia, and a small burr hole about 1 cm in diameter was made. The dura was opened, the brain surface exposed and a disposable Nashold Biopsy Needle (Integra Radionics, Burlington, MA, USA) introduced immediately below the cortical surface. A biopsy (0.9 × 10 mm) was then aspirated through the needle. Then, a solid ICP sensor (Codman MicroSensor™, Johnson & Johnson, Raynham, MA, USA) was tunneled subcutaneously, zeroed against the atmospheric pressure and introduced 1–2 cm into the frontal cortex parenchyma via the small opening established by the biopsy. The overnight monitoring and subsequent analysis of ICP scores was undertaken as previously described in detail (Eide & Sorteberg, 2010, 2016).

2.5 | Post-embedding transmission electron microscopy (TEM)

The tissue for TEM comprised the cortical layers 4, 5, and 6. We have previously reported the detailed technical procedures for the handling, processing, and analysis of the frontal cortex biopsies (Eide & Hansson, 2018; Eidsvaag et al., 2017). In short, the sampled brain material was immediately taken care of, dissected and fixed by immersion in 0.1 M phosphate buffer containing 4% paraformaldehyde and 0.25% glutaraldehyde and cut into small specimens (typically 0.5 × 0.5 × 1 mm). The EM specimens were subjected to freeze substitution and infiltration in Lowicryl HM20 resin (Polysciences Inc., Warrington, PA, USA, Cat 15924) (Schwarz & Humbel, 1989). Sections of 80 nm thicknesses were cut using a Reichert ultramicrotome (Reichert Techn., Wien, Austria), mounted on nickel grids and further processed counterstained with 1% uranyl acetate and 0.3% lead citrate for ultrastructure analysis.

2.6 | Quantitative measurements

A FEI Tecnai™ 12 transmission electron microscope (FEI Company, Hillsboro, OR, USA) was used for recording of EM at different magnifications of ×43,000, ×26,500, ×20,500, ×11,500, ×9,900, ×8,200, ×6,000, and ×4,200. The micrographs were saved as 2,048 × 2,048 pixels. Eight bit images were subsequently analyzed using a MATLAB-based toolbox (Enger, 2017), designed for evaluation of mitochondrial area, as previously described (Hasan-Olive et al., 2019). The respective lengths (nm) per pixel for different magnifications of EMs were calculated for MATLAB input prior to analyzing the images. Then the manually drawn areas over visible mitochondria were subject to analysis.

Morphological assessment of capillaries was done as previously described (Eidsvaag et al., 2017). In short, a capillary was identified as a small caliber (<8 μm) vessel bordered by a single layer of endothelial cells with an abluminal basal membrane. Pericytes were identified as cellular structures within the basal membrane abluminal to the endothelial cells (i.e., with basal membrane on both luminal and abluminal side). Astrocytic perivascular endfoot processes were identified as membrane enclosed structures with relatively low electron density facing toward the basal membrane of the vessel's endothelial cells or the interspersed pericytes.

Only astrocytic endfoot processes toward capillaries (not arterioles or venules) and the soma and pre- and postsynaptic terminals of neurons were analyzed. The mitochondria were fewer in number within the endfoot processes, as compared with neuronal compartments, although the shape and size of mitochondria in endfoot end were similar to mitochondria in the neuronal compartments.

2.6.1 | Normal, pathological, and clustered mitochondria

The MATLAB toolbox (Enger, 2017) comprises extended algorithmic features for analyzing number of normal and pathological

mitochondria per patient, and area of mitochondria per soma in each patient. We used the MATLAB toolbox to categorize normal, pathological, and clustered mitochondria, as previously described (Hasan-Olive, et al., 2019).While normal mitochondria are regular shaped with intact matrix and cristae and an electron dense appearance on TEM, damaged and dysfunctional mitochondria are irregular in shape with a swollen appearance, disruption of the cristae and a less electron dense appearance on TEM (Baloyannis, 2006; Kumar et al., 2016; Lauritzen et al., 2016; Solenski et al., 2002). Clustering of mitochondria is indicative of defect "mitophagy" (Martin-Maestro et al., 2016). In this present study, we differentiated normal, pathological, and clustered mitochondria according to the following criteria:

- Normal mitochondria: They were dark and electron dense, regular shaped and with intact matrix and cristae.
- Pathological mitochondria: They were light and less electron dense, with irregular shape and a swollen appearance, and with less intact matrix cristae.
- Clustered mitochondria were irregularly electron dense, with less intact cristae, and irregular shaped, and clumped and aggregated. The clustered mitochondria were only examined in the neuronal soma.

2.6.2 | Autophagic vacuoles

The number, area, and fraction of autophagic vacuoles were examined in the soma of neurons using the MATLAB toolbox (Enger, 2017).

2.6.3 | Mitochondria-ER contact sites (MERCs)

The mitochondria–endoplasmic reticulum (ER) contact sites (MERCs) were also measured using the MATLAB toolbox for analyses of length on electron micrographs. The length of mitochondria/ER contact was measured as the length of the ER projected onto the mitochondrion. The shortest distances between ER and mitochondria were measured at equal distances along this contact site. For each individual, the length of mitochondria/ER contact was measured and the average distance between mitochondria and ER determined for this particular length. The average of these regularly spaces measurements of distance mitochondria to ER was referred to as MERCs distance. Shortened distance between mitochondria and ER is considered as evidence of pathology (Leal et al., 2018; Stacchiotti et al., 2018).

2.6.4 | Postsynaptic density (PSD)

Electron micrographs with clearly visible synapses were recorded randomly, and postsynaptic densities (PSDs) identified in dendritic spines were measured by their length of electron dense appearance, forming asymmetric synapses with nerve terminals. The MATLAB toolbox was used for the analysis of length of PSD (expressed in μm) on electron micrographs.

2.7 | Light microscopy

The light microscopic immunohistochemistry and semi-quantitative assessment of glial fibrillary acidic protein (GFAP) has previously been described in detail (Eide et al., 2016; Eide & Hansson, 2018).

2.8 | Statistical analysis

Statistical analyses were performed using the SPSS software version 25 (IBM Corporation, Armonk, NY, USA). The data were pooled for each individual and presented as mean ± standard deviation. Differences between continuous data were determined using independent samples *t*-tests or Mann–Whitney *U*-test when distribution of data was uneven. Differences between categorical data were determined using Pearson Chi-square test. Correlation between variables was determined using Pearson correlation coefficient. Statistical significance was accepted at the 0.05 level (two-tailed).

3 | RESULTS

3.1 | Patients and biopsy samples

To evaluate mitochondrial morphology in astrocytic endfeet, we examined nine REF individuals and eight IIH patients. The demographic data are presented in Table 1. The average age and gender distribution of the patient cohorts were comparable. As expected, the BMI was significantly higher in the IIH cohort. Furthermore, headache and visual failure occurred more often in IIH.

The biopsies from REF subjects were from the gray matter of temporal cortex in four epilepsy cases, frontal cortex in three patients (two aneurysm, one tumor), parieto-occipital cortex in one epilepsy case, and from the occipital cortex in another epilepsy patient. The biopsies from the nine IIH patients were from gray matter of frontal cortex.

3.2 | Mitochondria in astrocytic endfoot processes

Analysis of mitochondria in astrocytic endfoot processes was based on 18.0 ± 8.2 and 14.0 ± 5.7 astrocytic endfoot processes per patient in the REF and IIH cohorts, respectively. In these cohorts, the total sampled area of endfoot processes were 2,040,461 ± 1,009,156 and 1,704,121 ± 771,391 nm^2, respectively.

Representative mitochondria in astrocytic endfoot processes of REF and IIH subjects are shown in Figure 1 (see also Figure S1). As shown in Table 2, in astrocytic endfoot processes of IIH patients, the number of pathological mitochondria was significantly increased, accompanied by a reduction in the number of normal mitochondria. Furthermore, the area of pathological mitochondria in astrocytic endfeet was double that seen in REF subjects.

TABLE 1 Demographic, clinical, management, and outcome data of the IIH and REF groups

	REF	IIH	Significance
Number	9	8	
Gender (F/M)	4/5	5/3	$X^2(1) = 0.544$, $p = 0.457$
Age (years)	42.7 ± 18.6	36.4 ± 13.7	$t(15) = 0.783$, $p = 0.446$
BMI (kg/m^2)	24.9 ± 4.2	32.8 ± 8.2	$t(15) = 2.521$, $p = 0.024$
Co-morbidity			
Arterial hypertension, *n* (%)	2 (22.2%)	0	
Diabetes mellitus, *n* (%)	0	0	
Pre-operative symptoms			
Duration of symptoms (years)	10.6 ± 10.5	3.3 ± 2.1	$t(15) = 1.928$, $p = 0.073$
Headache, *n* (%)	3 (33.3%)	8 (100%)	$X^2(1) = 8.242$, $p = 0.004$
Visual disturbances, *n* (%)	0 (0%)	6 (75%)	$X^2(1) = 10.432$, $p = 0.001$
Dizziness, *n* (%)	4 (44.4%)	1 (12.5%)	$X^2(1) = 2.082$, $p = 0.149$
Tinnitus, *n* (%)	1 (11.1%)	2 (25%)	$X^2(1) = 1.639$, $p = 0.200$
Cognitive impairment, *n* (%)	3 (33.3%)	3 (37.5%)	$X^2(1) = 0.032$, $p = 0.858$
ICP scores			
Mean ICP, average (mmHg)		13.4 ± 4.1	
Mean ICP, >15 mmHg (%)		33 ± 35	
MWA, average (mmHg)		5.9 ± 2.8	
MWA, >5 mmHg (%)		51 ± 32	
Management			
Shunt surgery, *n* (%)		6 (75%)	
Conservative, *n* (%)		2 (25%)	
Cranial surgery (epilepsy 6, aneurysm 2, tumor 1), *n* (%)	9 (100%)		
Outcome of treatment of IIH			
Headache			
Complete relief		2 (25%)	
Partial relief		3 (37.5%)	
No relief		3 (37.5%)	
Visual problems		2 (20%)	
Complete improvement		5 (30%)	
Partial improvement		3 (50%)	

Note: Categorical data presented as numbers; continuous data as mean ± standard deviation (*SD*). Independent samples *t* test for continuous data and Pearson chi-square test for categorical data.

Since reactive gliosis is a hallmark of many brain disorders, and that reactive gliosis is known to affect astrocytic endfoot protein expression, we wanted to assess the relationship between the number of pathological mitochondria and reactive gliosis in our biopsies. All biopsies were cut in half and one was assessed by EM and the other half was investigated by immunohistochemistry. The numbers of normal and pathological mitochondria correlated significantly with the degree of astrogliosis assessed by immunohistochemistry in the duplicate samples from the same patient. With increasing degree of

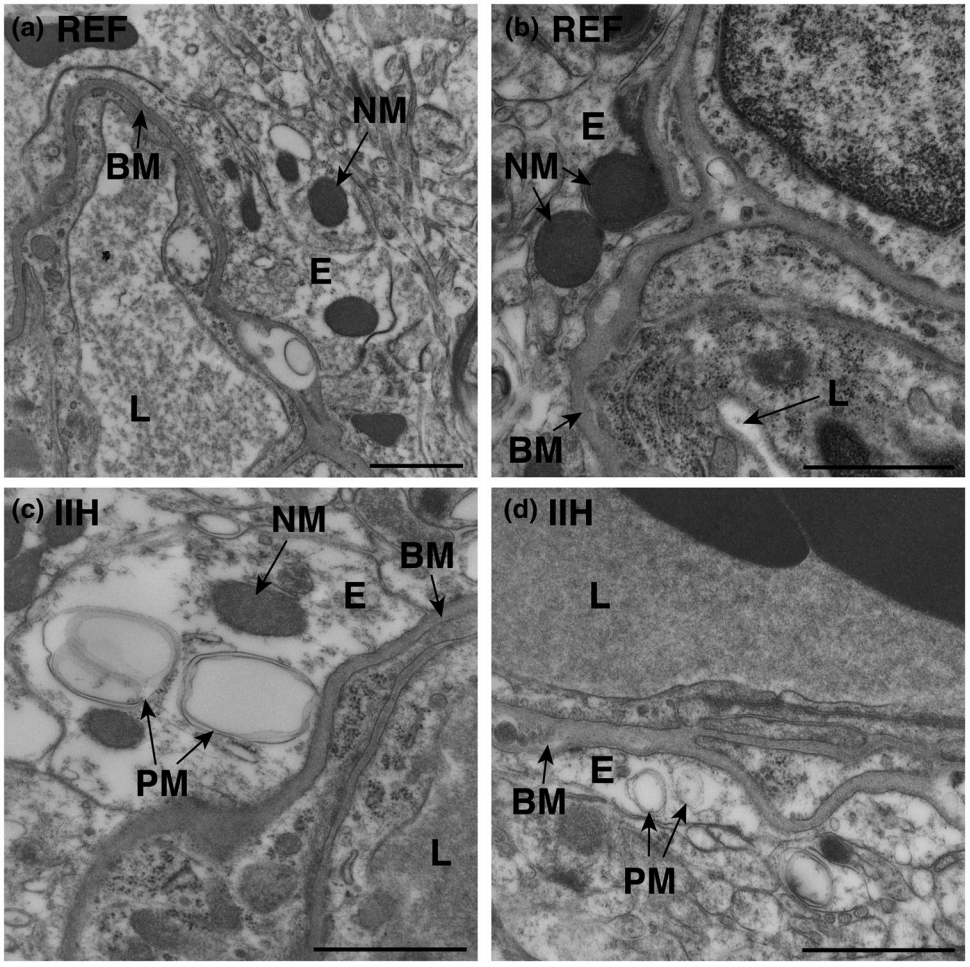

FIGURE 1 Increased occurrence of pathological mitochondria in astrocytic perivascular endfeet of idiopathic intracranial hypertension (IIH) patients. Electron micrographs demonstrate (a,b) normal mitochondria (NM) in the astrocytic endfeet of reference (REF) individuals, and (c,d) pathological mitochondria (PM) in IIH subjects. Magnifications: (a) 16,500×, scale bar 1 μm; (b–d) 26,500×, scale bar 500 nm. BM, basement membrane; E, endfoot process; L, lumen of capillary

TABLE 2 Normal and pathological mitochondria in astrocytic endfeet of REF and IIH subjects

	REF ($n = 9$)	IIH ($n = 8$)	Significance
Normal mitochondria			
Number of normal mitochondria per astrocytic endfoot process (n)	18.4 ± 9.4	7.0 ± 4.5	$t(12) = 2.901$, $p = 0.013$
Area of normal mitochondria per endfoot processes (nm^2)	132,672 ± 48,824	116,204 ± 51,446	$t(12) = 0.614$, $p = 0.550$
Pathological mitochondria			
Number of pathological mitochondria per astrocytic endfoot process (n)	0.43 ± 0.79	3.14 ± 3.08	$t(12) = 2.260$, $p = 0.043$
Area of pathological mitochondria per endfoot processes (nm^2)	28,903 ± 49,387	58,313 ± 46,878	$t(12) = 1.143$, $p = 0.275$

Note: Data presented as mean ± standard deviation (*SD*). Significant differences between continuous variables were determined by independent samples *t* test.

astrogliosis, evaluated by GFAP immunoreactivity (see Figure S2), the number of normal mitochondria was significantly reduced (Figure 2a). The number of pathological mitochondria tended to increase although significance level depended on statistical test (Figure 2b). To conclude, our data demonstrate pathological mitochondria in astrocytic endfeet in IIH, and it seems as degree of mitochondrial pathology correlates with the degree of astrogliosis.

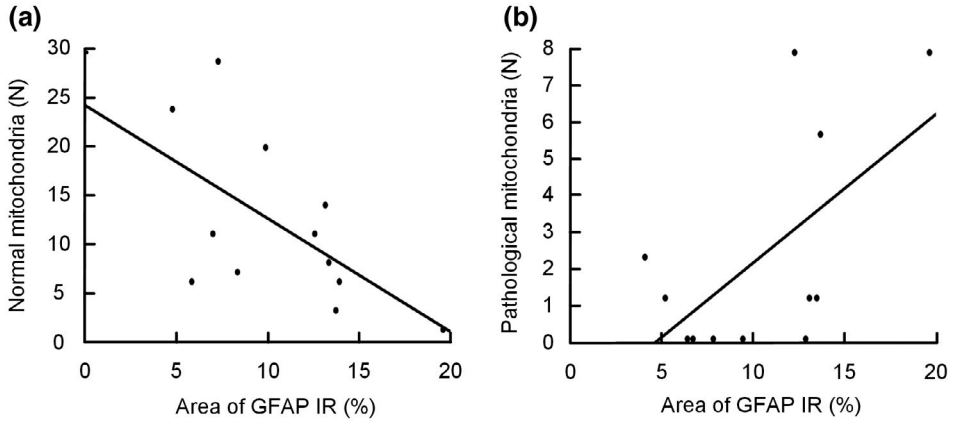

FIGURE 2 Association between degree of astrogliosis and number of normal and pathological mitochondria in astrocytic perivascular endfoot processes. (a) The correlation between number of normal mitochondria in astrocytic endfoot processes and percentage glial fibrillary acidic protein (GFAP) IR ($n = 12$; Spearman's correlation: −0.59, $p = 0.042$. Pearson correlation: −0.59, $p = 0.042$). (b) The correlation between number of pathological mitochondria in astrocytic endfoot processes and degree of astrogliosis ($n = 12$; Spearman's correlation: 0.41, $p = 0.190$. Pearson correlation: 0.604; $p = 0.037$)

3.3 | Mitochondria in neurons

Next, in light of our findings of pathological mitochondria in astrocytic endfeet, and the cognitive decline of patients with IIH, we studied mitochondrial characteristics of neurons. For analysis of mitochondria in neurons, we examined 12.7 ± 6.5 and 9.4 ± 6.1 soma per patient in the REF and IIH cohorts, respectively. Cytoplasmic area in these cohorts were 16,982,978 ± 5,335,206 and 14,267,563 ± 8,219,343 nm^2, respectively. In neuronal somata, the number and area of normal and pathological mitochondria were similar in the two groups (Table 3). Examples of pathological mitochondria in neuronal soma of IIH cases are presented in Figure S3.

Clustered mitochondria are considered pathological, and were mostly found in IIH patients: the number and area of clustered mitochondria were about fivefold higher in IIH than REF subjects, but the difference was not significant, as the total number of clustered mitochondria was low. Clustered mitochondria in IIH subjects are shown in Figures S4 and S5.

Another measure indicative of mitochondria dysfunction in neuronal somata is the distance between mitochondria and the endoplasmic reticulum, the so-called MERCs (Giacomello & Pellegrini, 2016). In IIH patients, the MERCs distances were significantly reduced (Figure 3).

Moreover, accumulation of autophagy vacuoles is a sign of altered cellular clearance. We found autophagy vacuoles in 2/9 (22%) REF subjects and 4/8 (50%) IIH subjects. The area of autophagic vacuoles per soma was comparable between IIH than REF subjects (184,362 ± 213,425 and 125,393 ± 342,944 nm^2). Examples of autophagic vacuoles are shown in Figure S6.

In REF and IIH cohorts, we analyzed 38.9 ± 24.6 and 56.5 ± 19.1 presynaptic terminals per patient (non-significant differences between patient cohorts). The areas of examined presynaptic terminals were 799,242 ± 216,666 and 578,592 ± 60,669 nm^2, respectively. In presynaptic terminals of IIH, we found significantly increased number and area of pathological mitochondria (Table 3).

The analysis of mitochondria in postsynaptic terminals was based on 35.9 ± 23.2 and 57.5 ± 19.1 postsynaptic terminals in REF and IIH subjects was, respectively, which included an area of 628,564 ± 208,871 and 373,637 ± 47,019 nm^2 postsynaptic terminals. In postsynaptic terminals of IIH subjects, the number of normal mitochondria was significantly reduced and the number and area of pathological mitochondria significantly increased (Table 3).

The length of the PSD, which is a measure of synaptic strength (Horn et al., 1985), was significantly reduced in IIH patients, as compared to REF individuals (Figure 4). The distance studied in the two cohorts was comparable.

4 | DISCUSSION

The main observations of this study were increased frequency of pathological mitochondria in perivascular astrocytic endfeet of IIH patients. The alterations correlated with the level of reactive astrogliosis in duplicate samples from the same patients. This study also shows altered mitochondrial structure in neurons, primarily revealed as altered MERCs in soma of IIH, and increased number of pathological mitochondria in the pre- and postsynaptic terminals of neurons. Moreover, PSD length was reduced in IIH.

The present observations of altered mitochondria phenotype cannot be referred to as age effects; given that the IIH patients were somewhat younger than the REF individuals. The finding of significantly increased BMI in IIH compares with the knowledge that IIH affects overweight people (Fric et al., 2017; Mollan et al., 2018).

The endfeet of the astrocytes completely ensheath the capillaries of the brain, contributing to maintenance of BBB function (Haddad-Tovolli et al., 2017), and 3D (3 dimensional) EM demonstrated bundles of mitochondria in the endfoot processes close to perivascular endfoot membrane (Mathiisen et al., 2010). It has been hypothesized

TABLE 3 Normal and pathological mitochondria in neurons of REF and IIH subjects

	REF ($n = 9$)	IIH ($n = 8$)	Significance
Neuronal soma			
Normal mitochondria			
Number of normal mitochondria per soma (*n*)	50.8 ± 31.2	37.1 ± 26.7	$t(14) = 0.921$, $p = 0.373$
Area of normal mitochondria per soma (nm^2)	134,348 ± 28,130	148,286 ± 81,386	$t(14) = 0.482$, $p = 0.637$
Pathological mitochondria			
Number of pathological mitochondria per soma (*n*)	8.8 ± 11.2	20.5 ± 24.1	$t(15) = 1.313$, $p = 0.209$
Area of pathological mitochondria per soma (nm^2)	240,857 ± 85,877	179,493 ± 84,110	$t(10) = 1.250$, $p = 0.240$
Presynaptic terminals			
Normal mitochondria			
Number of normal mitochondria per presynaptic terminal (*n*)	25.6 ± 16.1	19.5 ± 12.8	$t(11) = 0.658$, $p = 0.524$
Area of normal mitochondria per presynaptic terminal (nm^2)	91,017 ± 32,840	86,311 ± 18,669	$t(11) = 0.264$, $p = 0.797$
Pathological mitochondria			
Number of pathological mitochondria per presynaptic terminal (*n*)	0.1 ± 0.3	4.3 ± 4.0	$t(11) = 3.242$, $p = 0.008$
Area of pathological mitochondria per presynaptic terminal (nm^2)	59,537 ± 178,611	130,097 ± 46,214	$t(11) = 0.761$, $p = 0.462$
Postsynaptic terminals			
Normal mitochondria			
Number of normal mitochondria per postsynaptic terminal (*n*)	6.1 ± 5.6	6.0 ± 3.5	$t(11) = 0.036$, $p = 0.970$
Area of normal mitochondria per postsynaptic terminal (nm^2)	160,597 ± 83,189	58,612 ± 68,869	$t(11) = 2.134$, $p = 0.056$
Pathological mitochondria			
Number of pathological mitochondria per postsynaptic terminal (*n*)	0	1.0 ± 1.2	$t(11) = 2.277$, $p = 0.044$
Area of pathological mitochondria per postsynaptic terminal (nm^2)	0	166,672 ± 233,199	$t(11) = 2.760$, $p = 0.019$

Note: Data presented as mean ± standard deviation (*SD*). Significant differences between continuous variables were determined by independent samples *t* test or Mann–Whitney *U*-test.

that endfeet may actively control flow of CSF into the parenchyma (Iliff et al., 2012). A seminal study demonstrated the properties of CSF transport through the parenchyma and coined this fluid circulation "the glymphatic circulation" as it was dependent on aquaporin-4—a key channel in the astrocytic endfeet (Iliff et al., 2012). The mechanisms by which glymphatic flow are regulated remains disputed. The present observations of pathological mitochondria in astrocytic endfeet could have consequences for endfoot regulation and signaling. It is tempting to hypothesize that the glymphatic flow may be affected in IIH patients.

While the prevailing concept about IIH highlights CSF disturbance and venous pressure as causes of increased ICP and symptoms of the disease (Mollan et al., 2016, 2018), pathological processes within the brain parenchyma have received less attention. In cortical gray matter of IIH patients, we have previously demonstrated patchy astrogliosis (Eide et al., 2016), which is accompanied with changes in the basement membrane and pericytes of the cerebral capillaries (Eidsvaag et al., 2018), and leakage of blood proteins over the BBB of the capillaries (Hasan-Olive, et al., 2019). The present data add to these findings, and further suggest that alterations at the neurogliovascular interface are associated with astrogliosis.

The neurogliovascular interface, or neurogliovascular units, comprising interacting neurons, astrocytic endfeet, and blood vessels (including smooth muscle cells and pericytes), emphases the critical symbiotic relationship and interactions between the cells in the brain and its blood vessels (Iadecola, 2017). The increased prevalence of pathological and a concomitant reduction of normal mitochondria in the cells constituting the neurogliovascular interface in IIH add to the likelihood of impaired signaling and function of the neurogliovascular interface, and possibly affect blood flow regulation in these patients. It must be underlined that we previously have reported a range of other abnormalities in the structures forming the neurogliovascular units in IIH (Eide et al., 2016; Eidsvaag et al., 2018; Hasan-Olive, et al., 2019). Further studies are warranted to elucidate the potential impact of the multitude of abnormalities seen in IIH on blood flow and CSF circulation.

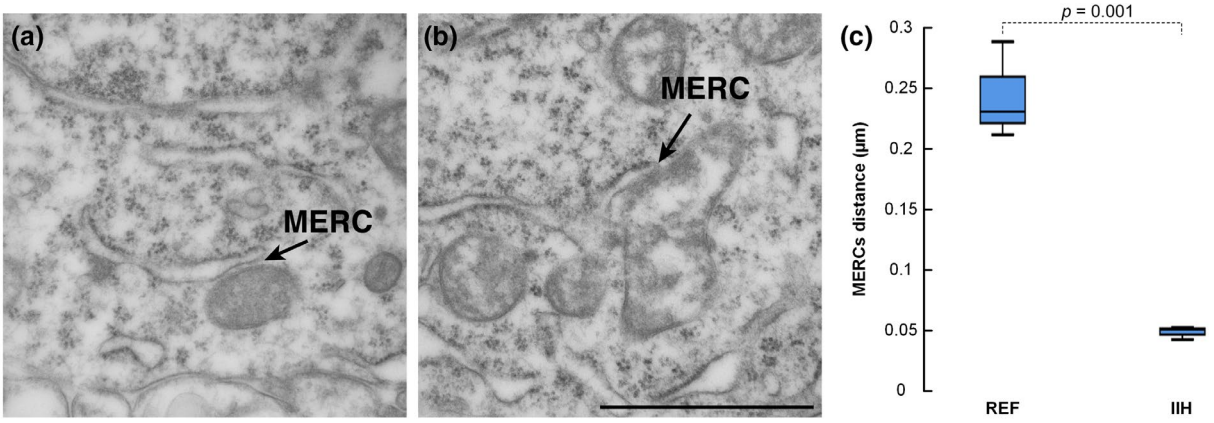

FIGURE 3 Reduced distance between mitochondria and endoplasmic reticulum in idiopathic intracranial hypertension (IIH). (a) EM reveals the endoplasmic reticulum (ER) and normal mitochondria in a reference (REF) individual, including visualization of the mitochondria–ER contact sites (MERCs). (b) The MERCs is shown in an IIH patient. Scale bar 1 µm. (c) The MERCs distance in IIH was 5.2-fold shorter than in REF individuals (0.24 ± 0.04 vs. 0.05 ± 0.005 µm; $p = 0.001$; independent samples t test, $t = 8.391$, $df = 4$). The length of ER was similar in the REF and IIH patients (0.67 ± 0.30 vs. 0.92 ± 0.40 µm, $p = 0.422$; independent samples t test, $t = -0.893$, $df = 4$). Error bars are 95% CI. Magnification 43,000×; scale bar 500 nm [Color figure can be viewed at wileyonlinelibrary.com]

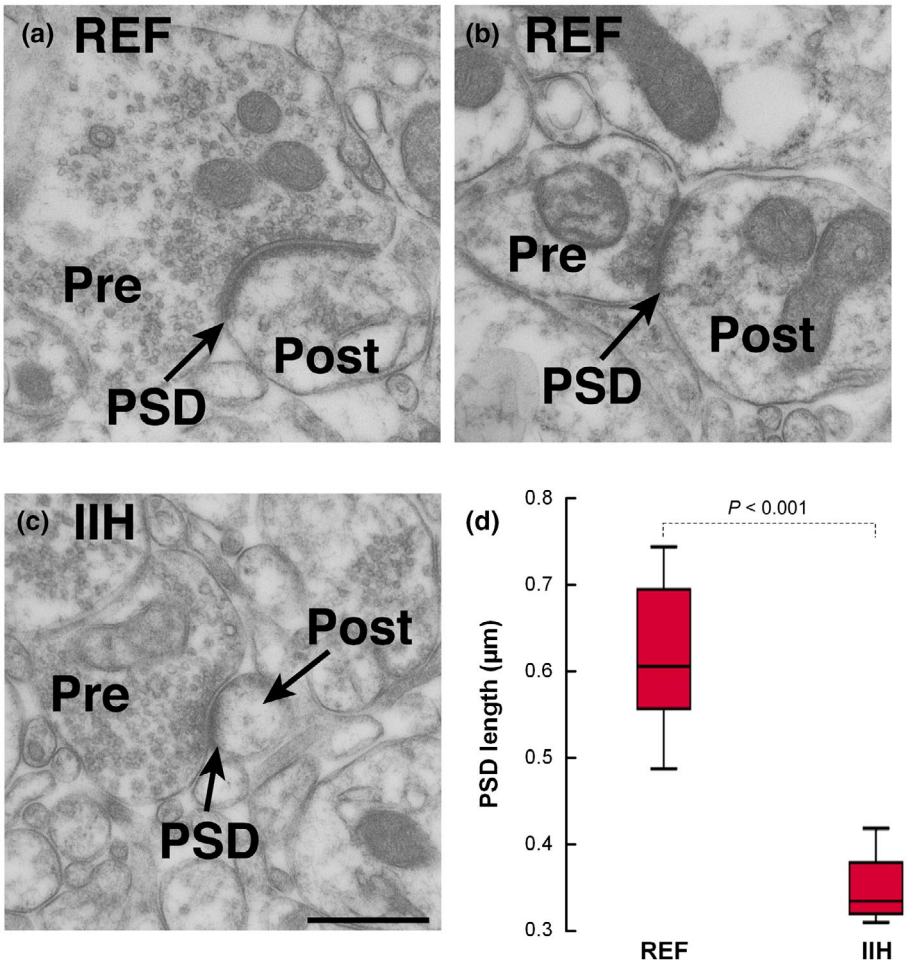

FIGURE 4 Reduced postsynaptic density (PSD) length in idiopathic intracranial hypertension (IIH) compared to reference (REF). (a,b) EM showing PSD in a REF subject, revealing the pre- (Pre) and postsynaptic (Post) terminals. (c) PSD in an individual with IIH, revealed as length of PSD. (d) The PSD length was nearly twofold higher in REF than IIH patients (0.61 ± 0.09 vs. 0.34 ± 0.05 µm ($p < 0.001$; independent samples t test, $t = 5.391$, $df = 11$). Error bars are 95% CI. Magnification 43,000×; scale bar 500 nm [Color figure can be viewed at wileyonlinelibrary.com]

It is hypothesized that obesity may play a role in the development of IIH (Mollan et al., 2016), although the mechanisms at play are elusive. In accordance with this hypothesis, in women with IIH, low-energy diet was accompanied with lowered ICP, reduced papilledema, and less severe symptoms (Sinclair et al., 2010). Moreover, reversible brain changes were seen with high-fat diet (Berkseth et al., 2014; Haltia et al., 2007; Hao et al., 2016). As astrogliosis can be triggered by obesity (Hao et al., 2016; Horvath et al., 2010), it is tempting to speculate that the increased astrogliosis and increased numbers of pathological mitochondria in IIH that we observe can be associated with obesity. However, astrogliosis may also occur secondary to various noxious agents, chemokines and cytokines, trauma, infections and inflammations (Oberheim et al., 2012; Verkhratsky & Butt, 2013; Winters & Kleinschmidt-Demasters, 2015). Accordingly, astrogliosis in IIH could also be a response to BBB leakage of blood proteins (Hasan-Olive, et al., 2019), given that extravasated blood proteins are pro-inflammatory (Liebner et al., 2018; Zlokovic, 2008).

Astrocytes play a key role in brain metabolism and are critical for bridging the functional connection between neurons and capillaries (Howarth, 2014). Proper mitochondrial function is therefore crucial for proper metabolism of astrocytes. Given that mitochondrial dysfunction may be associated with reactive cortical astrogliosis (Fiebig et al., 2019), the present observations of altered mitochondria phenotype in perivascular astrocytic endfeet suggest altered cellular metabolism.

It is well accepted that IIH negatively affects brain function, illustrated by visual failure, reduced olfactory function, tinnitus, hearing loss and impaired cognitive function in IIH patients (Bershad et al., 2014; Jindal et al., 2009; Kharkar et al., 2011; Kunte et al., 2013; Mollan et al., 2016; Reitsma et al., 2015; Yri et al., 2014). The present results suggest a cellular basis contributing to this dysfunction by showing elevated number of pathological mitochondria in both pre- and postsynaptic terminals.

Sufficient number of functional mitochondria is a prerequisite to maintain synaptic function given the high-energy demand in the pre- and postsynaptic terminals (Hollenbeck, 2005; Yu & Yu, 2017). This is clearly evident in tissue from Alzheimer's disease patients that also exhibit an abnormal accumulation of defective mitochondria in the nerve terminals (Correia et al., 2015). Damaged and dysfunctional mitochondria in the distal regions of the neuron are normally transported retrograde to the soma where they are repaired through fission and fusion processes (Sheng & Cai, 2012; Twig & Shirihai, 2011). The observed increase of pathological mitochondria in nerve terminals hence suggests impaired mitochondrial trafficking.

Clustering of mitochondria is another pathological sign. Overexpression of hyperphosphorylated tau (HPτ) causes increased mitochondrial clustering in Alzheimer's disease (Ebneth et al., 1998). Moreover, massive clustering of mitochondria is observed in amyotrophic lateral sclerosis (ALS) (Shan et al., 2010; Xu et al., 2010).

Another sign of dysfunctional mitochondria in neurons was the observation in neuronal soma of shortened distance between mitochondria and ER, resulting in increased number of MERCs. Comparable observations have previously been done in individuals with the dementia subtype idiopathic normal pressure hydrocephalus (iNPH) (Hasan-Olive, et al., 2019; Leal et al., 2018). Similar to Alzheimer's disease, in individuals with iNPH there is deposition of amyloid-β and cellular neuro-fibrillary tangles of HPτ (Leal et al., 2018). There is accumulating evidence suggesting increased occurrence of MERCs in Alzheimer's disease (Martino Adami et al., 2019) and Parkinson's disease (Lee et al., 2019). In Alzheimer's disease, MERCs were associated with amyloid-β and HPτ accumulation (Cieri et al., 2018). It should be noted, however, that the structure and dynamics of MERCs are complex (Giacomello & Pellegrini, 2016). For example, loosening of contact sites was reported for other neurodegenerative diseases, for example, ALS (Paillusson et al., 2016).

Traditionally, it has not been thought that IIH is accompanied with cognitive impairment. It is, however, our clinical experience that several of the affected individuals report subjective cognitive impairment. Several studies have reported cognitive decline in IIH patients (Kharkar et al., 2011; Yri et al., 2014). As the size of the PSD is a marker of synaptic strength, our finding of reduced PSD lengths could highlight the pathophysiological changes at play.

Brain tissue is prone to rapid degradation upon loss of blood flow, and therefore autopsy are rarely suitable for detailed analyses of subcellular structures (Hasan-Olive, et al., 2019; Verkhratsky & Butt, 2013). In the present study, proper preservation of mitochondria, autophagic vacuoles, cytoskeleton, and endoplasmic reticulum was of critical importance to enable mapping of any divergent ultrastructure of neurons and astrocytes in the human brain biopsies. To preserve the brain tissue as best as possible, all biopsies were immediately taken care of at the operating room, inspected, dissected (typically $0.5 \times 0.5 \times 1$ mm), and fixed by immersion within a few minutes after the surgery. The subsequent processing was standardized. We are hence confident that the structural changes observed are reproducible and reliable.

It should be noted that obtaining proper control tissue for such a study as this one is challenging as one cannot subject healthy controls to brain biopsies. Hence, our REF individuals are not healthy controls in all respects, but rather patients undergoing therapeutic procedures for other brain disorders. For instance, six of the nine patients had long-lasting epilepsy that could affect our results. Even so, our reference tissue was presumably healthy tissue removed as part of the therapeutic procedure.

5 | CONCLUSIONS

The present data demonstrate altered mitochondrial morphology in perivascular astrocytic endfeet and neurons of IIH patients, extending previous findings of substantial alterations at the glia-vascular interface of IIH subjects. Our results further suggest that IIH not only involves CSF disturbance but also involves pathological changes at the cellular level within the brain. Likely, our findings are signs of ongoing neurodegeneration, but could also be a more proximal cause for the disorder. Further studies are needed to fully elucidate the underpinnings of the disease.

DECLARATION OF TRANSPARENCY

The authors, reviewers and editors affirm that in accordance to the policies set by the *Journal of Neuroscience Research*, this manuscript presents an accurate and transparent account of the study being reported and that all critical details describing the methods and results are present.

ACKNOWLEDGMENTS

This work was supported by grants from Health South-East, Norway (grants 2012016 and 2016027). The authors thank Are Hugo Pripp, PhD, Department of Biostatistics, Epidemiology and Health Economics, Oslo University Hospital, Oslo, for statistical help during preparation of the paper.

CONFLICT OF INTEREST

The authors disclose no conflict of interest.

AUTHOR CONTRIBUTIONS

Conceptualization and Design, P.K.E., M.M.H.O., and R.E.; *Investigation*, M.M.H.O., P.K.E., and R.E.; *Formal Analysis*, M.M.H.O., P.K.E., and R.E.; *Visualization*, M.M.H.O., P.K.E., and R.E.; *Supervision*, P.K.E. and R.E.; *Administration*, P.K.E. and R.E.; *Writing – Original Draft*, P.K.E.; *Writing – Review & Editing*, P.K.E., M.M.H.O., H.A.H., and R.E.; *Approval of the Final Manuscript*, P.K.E., M.M.H.O., H.A.H., and R.E.; *Correspondence and Material Requests*, P.K.E.

PEER REVIEW

The peer review history for this article is available at https://publons.com/publon/10.1002/jnr.24743.

DATA AVAILABILITY STATEMENT

The data that support the findings of this study are available from the corresponding author upon reasonable request.

ORCID

Per Kristian Eide https://orcid.org/0000-0001-6881-9280

REFERENCES

Albuquerque, F. C., Dashti, S. R., Hu, Y. C., Newman, C. B., Teleb, M., McDougall, C. G., & Rekate, H. L. (2011). Intracranial venous sinus stenting for benign intracranial hypertension: Clinical indications, technique, and preliminary results. *World Neurosurgery*, *75*, 648–652. https://doi.org/10.1016/j.wneu.2010.11.012

Amiry-Moghaddam, M., & Ottersen, O. P. (2003). The molecular basis of water transport in the brain. *Nature Reviews Neuroscience*, *4*, 991–1001. https://doi.org/10.1038/nrn1252

Ball, A. K., & Clarke, C. E. (2006). Idiopathic intracranial hypertension. *Lancet Neurology*, *5*, 433–442. https://doi.org/10.1016/S1474-4422(06)70442-2

Baloyannis, S. J. (2006). Mitochondrial alterations in Alzheimer's disease. *Journal of Alzheimer's Disease*, *9*, 119–126. https://doi.org/10.3233/JAD-2006-9204

Berkseth, K. E., Guyenet, S. J., Melhorn, S. J., Lee, D., Thaler, J. P., Schur, E. A., & Schwartz, M. W. (2014). Hypothalamic gliosis associated with high-fat diet feeding is reversible in mice: A combined immunohistochemical and magnetic resonance imaging study. *Endocrinology*, *155*, 2858–2867. https://doi.org/10.1210/en.2014-1121

Bershad, E. M., Urfy, M. Z., Calvillo, E., Tang, R., Cajavilca, C., Lee, A. G., Venkatasubba Rao, C. P., Suarez, J. I., & Chen, D. (2014). Marked olfactory impairment in idiopathic intracranial hypertension. *Journal of Neurology, Neurosurgery and Psychiatry*, *85*, 959–964. https://doi.org/10.1136/jnnp-2013-307232

Boulay, A.-C., Saubaméa, B., Adam, N., Chasseigneaux, S., Mazaré, N., Gilbert, A., Bahin, M., Bastianelli, L., Blugeon, C., Perrin, S., Pouch, J., Ducos, B., Le Crom, S., Genovesio, A., Chrétien, F., Declèves, X., Laplanche, J.-L., & Cohen-Salmon, M. (2017). Translation in astrocyte distal processes sets molecular heterogeneity at the gliovascular interface. *Cell Discovery*, *3*, 17005. https://doi.org/10.1038/celldisc.2017.5

Cieri, D., Vicario, M., Vallese, F., D'Orsi, B., Berto, P., Grinzato, A., Catoni, C., De Stefani, D., Rizzuto, R., Brini, M., & Calì, T. (2018). Tau localises within mitochondrial sub-compartments and its caspase cleavage affects ER-mitochondria interactions and cellular Ca(2+) handling. *Biochimica et Biophysica Acta (BBA) - Molecular Basis of Disease*, *1864*, 3247–3256. https://doi.org/10.1016/j.bbadis.2018.07.011

Correia, S. C., Resende, R., Moreira, P. I., & Pereira, C. M. (2015). Alzheimer's disease-related misfolded proteins and dysfunctional organelles on autophagy menu. *DNA and Cell Biology*, *34*, 261–273. https://doi.org/10.1089/dna.2014.2757

Curry, W. T. Jr., Butler, W. E., & Barker, F. G., 2nd. (2005). Rapidly rising incidence of cerebrospinal fluid shunting procedures for idiopathic intracranial hypertension in the United States, 1988–2002. *Neurosurgery*, *57*, 97–108.

Dandy, W. E. (1937). Intracranial pressure without brain tumor: diagnosis and treatment. *Annals of Surgery*, *106*, 492–513. https://doi.org/10.1097/00000658-193710000-00002

Ebneth, A., Godemann, R., Stamer, K., Illenberger, S., Trinczek, B., Mandelkow, E.-M., & Mandelkow, E. (1998). Overexpression of tau protein inhibits kinesin-dependent trafficking of vesicles, mitochondria, and endoplasmic reticulum: Implications for Alzheimer's disease. *Journal of Cell Biology*, *143*, 777–794. https://doi.org/10.1083/jcb.143.3.777

Eid, T., Lee, T. S., Thomas, M. J., Amiry-Moghaddam, M., Bjornsen, L. P., Spencer, D. D., Agre, P., Ottersen, O. P., & de Lanerolle, N. C. (2005). Loss of perivascular aquaporin 4 may underlie deficient water and K+ homeostasis in the human epileptogenic hippocampus. *Proceedings of the National Academy of Sciences of the United States of America*, *102*, 1193–1198. https://doi.org/10.1073/pnas.0409308102

Eide, P. K., Eidsvaag, V. A., Nagelhus, E. A., & Hansson, H. A. (2016). Cortical astrogliosis and increased perivascular aquaporin-4 in idiopathic intracranial hypertension. *Brain Research*, *1644*, 161–175. https://doi.org/10.1016/j.brainres.2016.05.024

Eide, P. K., & Hansson, H. A. (2018). Astrogliosis and impaired aquaporin-4 and dystrophin systems in idiopathic normal pressure hydrocephalus. *Neuropathology and Applied Neurobiology*, *44*, 474–490. https://doi.org/10.1111/nan.12420

Eide, P. K., & Kerty, E. (2011). Static and pulsatile intracranial pressure in idiopathic intracranial hypertension. *Clinical Neurology and Neurosurgery*, *113*, 123–128. https://doi.org/10.1016/j.clineuro.2010.10.008

Eide, P. K., & Sorteberg, W. (2010). Diagnostic intracranial pressure monitoring and surgical management in idiopathic normal pressure hydrocephalus: A 6-year review of 214 patients. *Neurosurgery*, *66*, 80–91. https://doi.org/10.1227/01.NEU.0000363408.69856.B8

Eide, P. K., & Sorteberg, W. (2016). Outcome of surgery for idiopathic normal pressure hydrocephalus: Role of preoperative static and pulsatile intracranial pressure. *World Neurosurgery*, *86*, 186–193.e1. https://doi.org/10.1016/j.wneu.2015.09.067

Eidsvaag, V. A., Enger, R., Hansson, H. A., Eide, P. K., & Nagelhus, E. A. (2017). Human and mouse cortical astrocytes differ in aquaporin-4 polarization toward microvessels. *Glia*, *65*, 964–973. https://doi.org/10.1002/glia.23138

Eidsvaag, V. A., Hansson, H. A., Heuser, K., Nagelhus, E. A., & Eide, P. K. (2017). Brain capillary ultrastructure in idiopathic normal pressure hydrocephalus: Relationship with static and pulsatile intracranial pressure. *Journal of Neuropathology and Experimental Neurology*, *76*, 1034–1045. https://doi.org/10.1093/jnen/nlx091

Eidsvaag, V. A., Hansson, H. A., Heuser, K., Nagelhus, E. A., & Eide, P. K. (2018). Cerebral microvascular abnormalities in patients with idiopathic intracranial hypertension. *Brain Research*, *1686*, 72–82. https://doi.org/10.1016/j.brainres.2018.02.017

Enger, R. (2017). Automated gold particle quantification of immunogold labeled micrographs. *Journal of Neuroscience Methods*, *286*, 31–37. https://doi.org/10.1016/j.jneumeth.2017.05.018

Fiebig, C., Keiner, S., Ebert, B., Schaffner, I., Jagasia, R., Lie, D. C., & Beckervordersandforth, R. (2019). Mitochondrial dysfunction in astrocytes impairs the generation of reactive astrocytes and enhances neuronal cell death in the cortex upon photothrombotic lesion. *Frontiers in Molecular Neuroscience*, *12*, 40. https://doi.org/10.3389/fnmol.2019.00040

Fric, R., & Eide, P. K. (2017). Comparative observational study on the clinical presentation, intracranial volume measurements, and intracranial pressure scores in patients with either Chiari malformation Type I or idiopathic intracranial hypertension. *Journal of Neurosurgery*, *126*, 1312–1322. https://doi.org/10.3171/2016.4.JNS152862

Fric, R., Pripp, A. H., & Eide, P. K. (2017). Cardiovascular risk factors in Chiari malformation and idiopathic intracranial hypertension. *Brain and Behavior*, *7*, e00677. https://doi.org/10.1002/brb3.677

Friedman, D. I., & Jacobson, D. M. (2002). Diagnostic criteria for idiopathic intracranial hypertension. *Neurology*, *59*, 1492–1495. https://doi.org/10.1212/01.WNL.0000029570.69134.1B

Friesner, D., Rosenman, R., Lobb, B. M., & Tanne, E. (2011). Idiopathic intracranial hypertension in the USA: The role of obesity in establishing prevalence and healthcare costs. *Obesity Reviews*, *12*, e372–e380. https://doi.org/10.1111/j.1467-789X.2010.00799.x

Giacomello, M., & Pellegrini, L. (2016). The coming of age of the mitochondria-ER contact: A matter of thickness. *Cell Death and Differentiation*, *23*, 1417–1427. https://doi.org/10.1038/cdd.2016.52

Haddad-Tovolli, R., Dragano, N. R. V., Ramalho, A. F. S., & Velloso, L. A. (2017). Development and function of the blood-brain barrier in the context of metabolic control. *Frontiers in Neuroscience*, *11*, 224. https://doi.org/10.3389/fnins.2017.00224

Haltia, L. T., Viljanen, A., Parkkola, R., Kemppainen, N., Rinne, J. O., Nuutila, P., & Kaasinen, V. (2007). Brain white matter expansion in human obesity and the recovering effect of dieting. *Journal of Clinical Endocrinology and Metabolism*, *92*, 3278–3284. https://doi.org/10.1210/jc.2006-2495

Hao, S., Dey, A., Yu, X., & Stranahan, A. M. (2016). Dietary obesity reversibly induces synaptic stripping by microglia and impairs hippocampal plasticity. *Brain, Behavior, and Immunity*, *51*, 230–239. https://doi.org/10.1016/j.bbi.2015.08.023

Hasan-Olive, M. M., Enger, R., Hansson, H. A., Nagelhus, E. A., & Eide, P. K. (2019). Pathological mitochondria in neurons and perivascular astrocytic endfeet of idiopathic normal pressure hydrocephalus patients. *Fluids and Barriers of the CNS*, *16*, 39. https://doi.org/10.1186/s12987-019-0160-7

Hasan-Olive, M. M., Hansson, H. A., Enger, R., Nagelhus, E. A., & Eide, P. K. (2019). Blood-brain barrier dysfunction in idiopathic intracranial hypertension. *Journal of Neuropathology and Experimental Neurology*, *78*, 808–818. https://doi.org/10.1093/jnen/nlz063

Heuser, K., Eid, T., Lauritzen, F., Thoren, A. E., Vindedal, G. F., Tauboll, E., Gjerstad, L., Spencer, D. D., Ottersen, O. P., & Nagelhus, E. A. (2012). Loss of perivascular Kir4.1 potassium channels in the sclerotic hippocampus of patients with mesial temporal lobe epilepsy. *Journal of Neuropathology and Experimental Neurology*, *71*, 814–825.

Hollenbeck, P. J. (2005). Mitochondria and neurotransmission: Evacuating the synapse. *Neuron*, *47*, 331–333. https://doi.org/10.1016/j.neuron.2005.07.017

Horn, G., Bradley, P., & McCabe, B. J. (1985). Changes in the structure of synapses associated with learning. *Journal of Neuroscience*, *5*, 3161–3168. https://doi.org/10.1523/JNEUROSCI.05-12-03161.1985

Horvath, T. L., Sarman, B., Garcia-Caceres, C., Enriori, P. J., Sotonyi, P., Shanabrough, M., Borok, E., Argente, J., Chowen, J. A., Perez-Tilve, D., Pfluger, P. T., Bronneke, H. S., Levin, B. E., Diano, S., Cowley, M. A., & Tschop, M. H. (2010). Synaptic input organization of the melanocortin system predicts diet-induced hypothalamic reactive gliosis and obesity. *Proceedings of the National Academy of Sciences of the United States of America*, *107*, 14875–14880. https://doi.org/10.1073/pnas.1004282107

Howarth, C. (2014). The contribution of astrocytes to the regulation of cerebral blood flow. *Frontiers in Neuroscience*, *8*, 103. https://doi.org/10.3389/fnins.2014.00103

Iadecola, C. (2017). The neurovascular unit coming of age: A journey through neurovascular coupling in health and disease. *Neuron*, *96*, 17–42. https://doi.org/10.1016/j.neuron.2017.07.030

Iliff, J. J., Wang, M., Liao, Y., Plogg, B. A., Peng, W., Gundersen, G. A., Benveniste, H., Vates, G. E., Deane, R., Goldman, S. A., Nagelhus, E. A., & Nedergaard, M. (2012). A paravascular pathway facilitates CSF flow through the brain parenchyma and the clearance of interstitial solutes, including amyloid beta. *Science Translational Medicine*, *4*, 147ra111. https://doi.org/10.1126/scitranslmed.3003748

Jindal, M., Hiam, L., Raman, A., & Rejali, D. (2009). Idiopathic intracranial hypertension in otolaryngology. *European Archives of Oto-Rhino-Laryngology*, *266*, 803–806. https://doi.org/10.1007/s00405-009-0973-0

Kesler, A., Stolovic, N., Bluednikov, Y., & Shohat, T. (2014). The incidence of idiopathic intracranial hypertension in Israel from 2005 to 2007: Results of a nationwide survey. *European Journal of Neurology*, *21*, 1055–1059. https://doi.org/10.1111/ene.12442

Kharkar, S., Hernandez, R., Batra, S., Metellus, P., Hillis, A., Williams, M. A., & Rigamonti, D. (2011). Cognitive impairment in patients with pseudotumor cerebri syndrome. *Behavioural Neurology*, *24*, 143–148. https://doi.org/10.1155/2011/630475

Kirschen, G. W., Kéry, R., & Ge, S. (2018). The hippocampal neuro-glio-vascular network: Metabolic vulnerability and potential neurogenic regeneration in disease. *Brain Plasticity*, *3*, 129–144. https://doi.org/10.3233/BPL-170055

Kleinschmidt, J. J., Digre, K. B., & Hanover, R. (2000). Idiopathic intracranial hypertension. Relationship to depression, anxiety, and quality of life. *Neurology*, *54*, 319–324.

Kumar, R., Bukowski, M. J., Wider, J. M., Reynolds, C. A., Calo, L., Lepore, B., Tousignant, R., Jones, M., Przyklenk, K., & Sanderson, T. H. (2016). Mitochondrial dynamics following global cerebral ischemia. *Molecular and Cellular Neurosciences*, *76*, 68–75. https://doi.org/10.1016/j.mcn.2016.08.010

Kunte, H., Schmidt, F., Kronenberg, G., Hoffmann, J., Schmidt, C., Harms, L., & Goektas, O. (2013). Olfactory dysfunction in patients with idiopathic intracranial hypertension. *Neurology*, *81*, 379–382. https://doi.org/10.1212/WNL.0b013e31829c5c9d

Langer, J., Gerkau, N. J., Derouiche, A., Kleinhans, C., Moshrefi-Ravasdjani, B., Fredrich, M., Kafitz, K. W., Seifert, G., Steinhäuser, C., & Rose, C. R. (2017). Rapid sodium signaling couples glutamate uptake to breakdown of ATP in perivascular astrocyte endfeet. *Glia*, *65*, 293–308. https://doi.org/10.1002/glia.23092

Lauritzen, K. H., Hasan-Olive, M. M., Regnell, C. E., Kleppa, L., Scheibye-Knudsen, M., Gjedde, A., Klungland, A., Bohr, V. A., Storm-Mathisen, J., & Bergersen, L. H. (2016). A ketogenic diet accelerates neurodegeneration in mice with induced mitochondrial DNA

toxicity in the forebrain. *Neurobiology of Aging*, *48*, 34–47. https://doi.org/10.1016/j.neurobiolaging.2016.08.005

Leal, N. S., Dentoni, G., Schreiner, B., Kämäräinen, O.-P., Partanen, N., Herukka, S.-K., Koivisto, A. M., Hiltunen, M., Rauramaa, T., Leinonen, V., & Ankarcrona, M. (2018). Alterations in mitochondria-endoplasmic reticulum connectivity in human brain biopsies from idiopathic normal pressure hydrocephalus patients. *Acta Neuropathologica Communications*, *6*, 102. https://doi.org/10.1186/s40478-018-0605-2

Lee, J. H., Han, J. H., Kim, H., Park, S. M., Joe, E. H., & Jou, I. (2019). Parkinson's disease-associated LRRK2-G2019S mutant acts through regulation of SERCA activity to control ER stress in astrocytes. *Acta Neuropathologica Communications*, *7*, 68. https://doi.org/10.1186/s40478-019-0716-4

Liebner, S., Dijkhuizen, R. M., Reiss, Y., Plate, K. H., Agalliu, D., & Constantin, G. (2018). Functional morphology of the blood-brain barrier in health and disease. *Acta Neuropathologica*, *135*, 311–336. https://doi.org/10.1007/s00401-018-1815-1

Martin-Maestro, P., Gargini, R., Perry, G., Avila, J., & Garcia-Escudero, V. (2016). PARK2 enhancement is able to compensate mitophagy alterations found in sporadic Alzheimer's disease. *Human Molecular Genetics*, *25*, 792–806. https://doi.org/10.1093/hmg/ddv616

Martino Adami, P. V., Nichtová, Z., Weaver, D. B., Bartok, A., Wisniewski, T., Jones, D. R., Do Carmo, S., Castaño, E. M., Cuello, A. C., Hajnóczky, G., & Morelli, L. (2019). Perturbed mitochondria-ER contacts in live neurons that model the amyloid pathology of Alzheimer's disease. *Journal of Cell Science*, *132*, jcs229906. https://doi.org/10.1242/jcs.229906

Mathiisen, T. M., Lehre, K. P., Danbolt, N. C., & Ottersen, O. P. (2010). The perivascular astroglial sheath provides a complete covering of the brain microvessels: An electron microscopic 3D reconstruction. *Glia*, *58*, 1094–1103. https://doi.org/10.1002/glia.20990

Mollan, S. P., Ali, F., Hassan-Smith, G., Botfield, H., Friedman, D. I., & Sinclair, A. J. (2016). Evolving evidence in adult idiopathic intracranial hypertension: Pathophysiology and management. *Journal of Neurology, Neurosurgery and Psychiatry*, *87*, 982–992. https://doi.org/10.1136/jnnp-2015-311302

Mollan, S. P., Davies, B., Silver, N. C., Shaw, S., Mallucci, C. L., Wakerley, B. R., Krishnan, A., Chavda, S. V., Ramalingam, S., Edwards, J., Hemmings, K., Williamson, M., Burdon, M. A., Hassan-Smith, G., Digre, K., Liu, G. T., Jensen, R. H., & Sinclair, A. J. (2018). Idiopathic intracranial hypertension: Consensus guidelines on management. *Journal of Neurology, Neurosurgery and Psychiatry*, *89*, 1088–1100. https://doi.org/10.1136/jnnp-2017-317440

Mulligan, S. J., & MacVicar, B. A. (2004). Calcium transients in astrocyte endfeet cause cerebrovascular constrictions. *Nature*, *431*, 195–199. https://doi.org/10.1038/nature02827

Oberheim, N. A., Goldman, S. A., & Nedergaard, M. (2012). Heterogeneity of astrocytic form and function. *Methods in Molecular Biology*, *814*, 23–45.

Paillusson, S., Stoica, R., Gomez-Suaga, P., Lau, D. H. W., Mueller, S., Miller, T., & Miller, C. C. J. (2016). There's something wrong with my MAM; the ER-mitochondria axis and neurodegenerative diseases. *Trends in Neurosciences*, *39*, 146–157. https://doi.org/10.1016/j.tins.2016.01.008

Pekny, M., & Pekna, M. (2014). Astrocyte reactivity and reactive astrogliosis: Costs and benefits. *Physiological Reviews*, *94*, 1077–1098. https://doi.org/10.1152/physrev.00041.2013

Raoof, N., Sharrack, B., Pepper, I. M., & Hickman, S. J. (2011). The incidence and prevalence of idiopathic intracranial hypertension in Sheffield, UK. *European Journal of Neurology*, *18*, 1266–1268. https://doi.org/10.1111/j.1468-1331.2011.03372.x

Reitsma, S., Stokroos, R., Weber, J. W., & van Tongeren, J. (2015). Pediatric idiopathic intracranial hypertension presenting with sensorineural hearing loss. *Annals of Otology, Rhinology, and Laryngology*, *124*, 996–1001. https://doi.org/10.1177/0003489415591999

Schwarz, H., & Humbel, B. M. (1989). Influence of fixatives and embedding media on immunolabelling of freeze-substituted cells. *Scanning Microscopy*, *3*(Suppl. 3), 57–63.

Shan, X., Chiang, P. M., Price, D. L., & Wong, P. C. (2010). Altered distributions of Gemini of coiled bodies and mitochondria in motor neurons of TDP-43 transgenic mice. *Proceedings of the National Academy of Sciences of the United States of America*, *107*, 16325–16330. https://doi.org/10.1073/pnas.1003459107

Sheng, Z. H., & Cai, Q. (2012). Mitochondrial transport in neurons: Impact on synaptic homeostasis and neurodegeneration. *Nature Reviews Neuroscience*, *13*, 77–93. https://doi.org/10.1038/nrn3156

Sinclair, A. J., Burdon, M. A., Nightingale, P. G., Ball, A. K., Good, P., Matthews, T. D., Jacks, A., Lawden, M., Clarke, C. E., Stewart, P. M., Walker, E. A., Tomlinson, J. W., & Rauz, S. (2010). Low energy diet and intracranial pressure in women with idiopathic intracranial hypertension: Prospective cohort study. *BMJ*, *341*, c2701. https://doi.org/10.1136/bmj.c2701

Solenski, N. J., diPierro, C. G., Trimmer, P. A., Kwan, A. L., & Helm, G. A. (2002). Ultrastructural changes of neuronal mitochondria after transient and permanent cerebral ischemia. *Stroke*, *33*, 816–824. https://doi.org/10.1161/hs0302.104541

Stacchiotti, A., Favero, G., Lavazza, A., Garcia-Gomez, R., Monsalve, M., & Rezzani, R. (2018). Perspective: Mitochondria-ER contacts in metabolic cellular stress assessed by microscopy. *Cells*, *8*, 5. https://doi.org/10.3390/cells8010005

Twig, G., & Shirihai, O. S. (2011). The interplay between mitochondrial dynamics and mitophagy. *Antioxidants & Redox Signaling*, *14*, 1939–1951. https://doi.org/10.1089/ars.2010.3779

Verkhratsky, A., & Butt, A. (2013). *Glial physiology and pathophysiology*. Wiley-Blackwell.

Verkhratsky, A., & Nedergaard, M. (2018). Physiology of astroglia. *Physiological Reviews*, *98*, 239–389. https://doi.org/10.1152/physrev.00042.2016

Winters, H. V., & Kleinschmidt-Demasters, B. K. (2015). General pathology of the central nervous system. In S. Love, H. Budka, J. W. Ironside, & A. Perry (Eds.), *Greenfield's neuropathology* (9th ed., pp. 1–58). CRC Press.

Xu, Y.-F., Gendron, T. F., Zhang, Y.-J., Lin, W.-L., D'Alton, S., Sheng, H., Casey, M. C., Tong, J., Knight, J., Yu, X., Rademakers, R., Boylan, K., Hutton, M., McGowan, E., Dickson, D. W., Lewis, J., & Petrucelli, L. (2010). Wild-type human TDP-43 expression causes TDP-43 phosphorylation, mitochondrial aggregation, motor deficits, and early mortality in transgenic mice. *Journal of Neuroscience*, *30*, 10851–10859. https://doi.org/10.1523/JNEUROSCI.1630-10.2010

Yri, H. M., Fagerlund, B., Forchhammer, H. B., & Jensen, R. H. (2014). Cognitive function in idiopathic intracranial hypertension: A prospective case-control study. *British Medical Journal Open*, *4*, e004376. https://doi.org/10.1136/bmjopen-2013-004376

Yu, L., & Yu, Y. (2017). Energy-efficient neural information processing in individual neurons and neuronal networks. *Journal of Neuroscience Research*, *95*, 2253–2266.

Zlokovic, B. V. (2008). The blood-brain barrier in health and chronic neurodegenerative disorders. *Neuron*, *57*, 178–201. https://doi.org/10.1016/j.neuron.2008.01.003

SUPPORTING INFORMATION

Additional Supporting Information may be found online in the Supporting Information section.

FIGURE S1 Mitochondria in astrocytic endfoot processes of REF and IIH subjects

FIGURE S2 Gliofibrillary acidic protein immunoreactivity

FIGURE S3 Pathological mitochondria in neuronal soma of IIH patients

FIGURE S4 Increased occurrence of clustered mitochondria in REF and IIH subjects

FIGURE S5 Clustered mitochondria in neuronal soma of IIH subjects

FIGURE S6 Examples of autophagic vacuoles in REF and IIH

Transparent Peer Review Report

Transparent Science Questionnaire for Authors

How to cite this article: Eide PK, Hasan-Olive MM, Hansson H-A, Enger R. Increased occurrence of pathological mitochondria in astrocytic perivascular endfoot processes and neurons of idiopathic intracranial hypertension. *J Neurosci Res*. 2021;99:467–480. https://doi.org/10.1002/jnr.24743